Using electromagnetics to delineate proppant distribution in a hydraulically fractured reservoir

Lindsey J. Heagy*, Douglas W. Oldenburg
Geophysical Inversion Facility, University of British Columbia
lheagy@eos.ubc.ca

Collaborators:
Michael Wilt, Jiuping Chen
Schlumberger EMI Technology Center

Hydraulic Fracturing Process

- Used to create pathways for hydrocarbons to flow

Seal off section of wellbore

↓

Pump fluid to fracture rock

↓

Pump proppant to keep fractures open

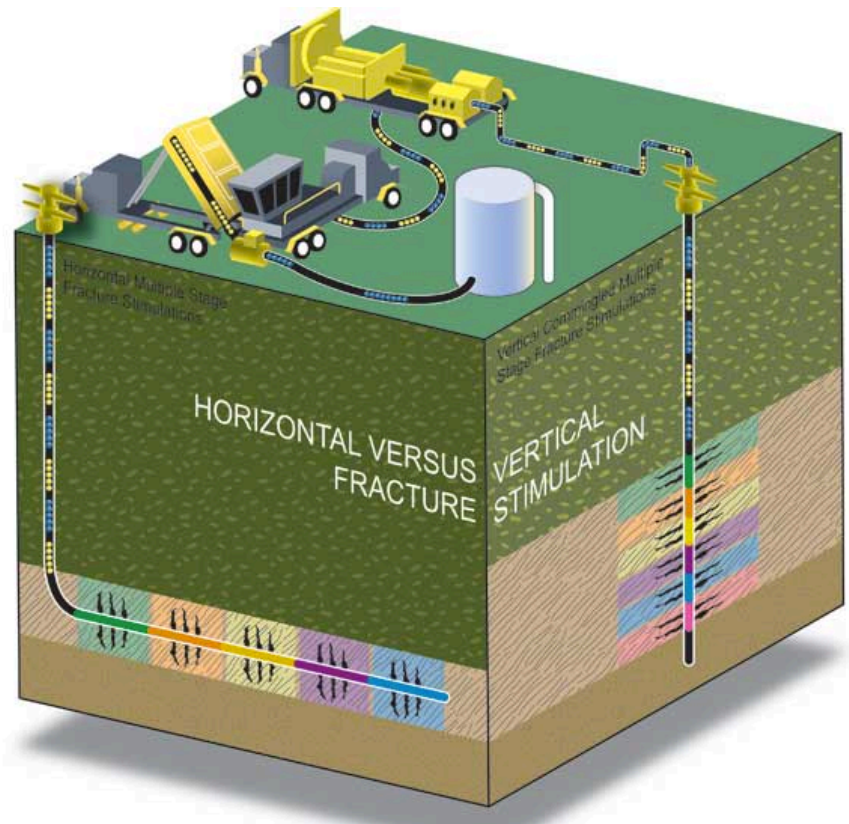

(National Energy Board, Canada, 2009)

Hydraulic Fracturing Process

- Used to create pathways for hydrocarbons to flow
- Completions parameters:
  - well spacing
  - stage spacing
  - volume of proppant
  - volume of fluid
  - pumping pressures
  - …

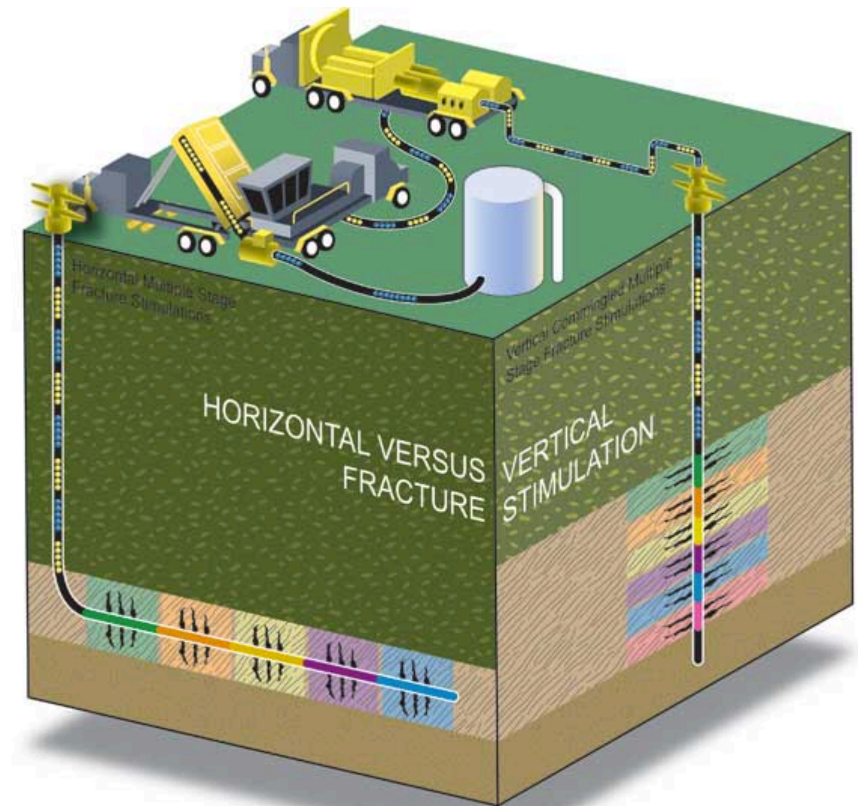

(National Energy Board, Canada, 2009)

Hydraulic Fracturing Process

- How do we optimize fracture completions?

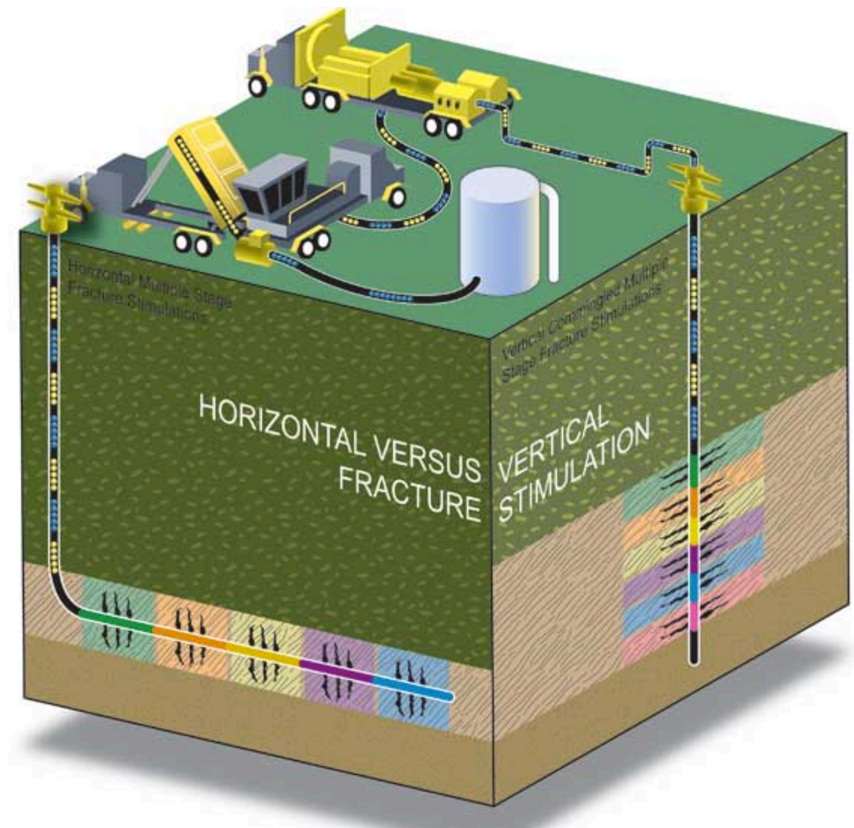

(National Energy Board, Canada, 2009)

Hydraulic Fracturing Process

- How do we optimize fracture completions?
- Before that…
  - need to understand impact on the reservoir
    - fracture geometry
    - production / injection behavior
    - distribution of proppant

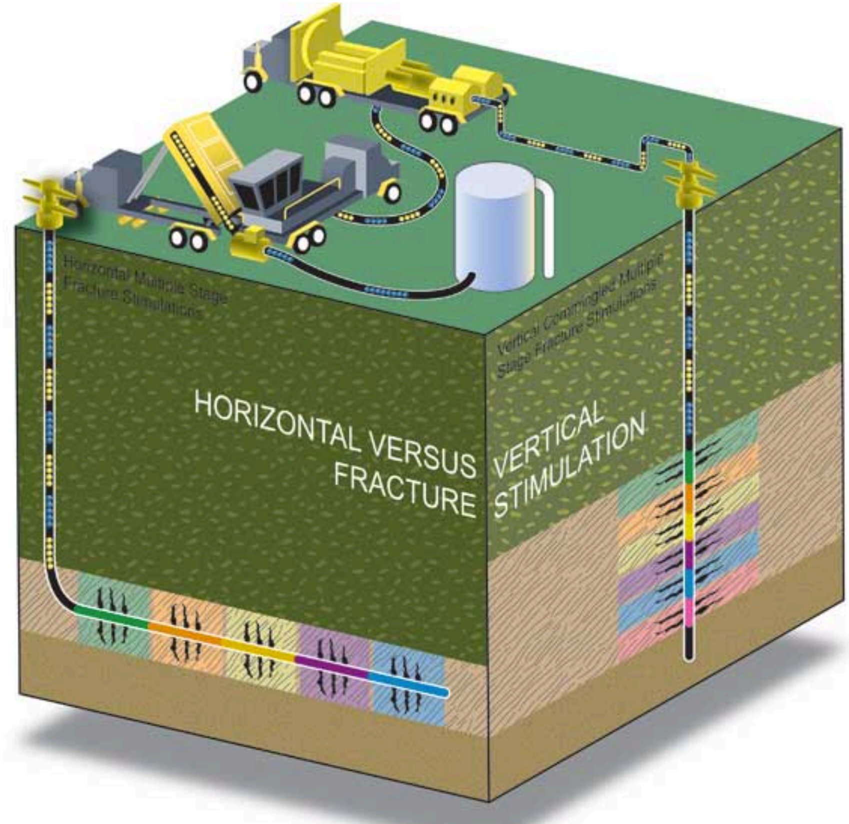

(National Energy Board, Canada, 2009)

Hydraulic Fracturing Process

- How do we optimize fracture completions?
- Before that…
  - need to understand impact on the reservoir
    - fracture geometry
    - production / injection behavior
    - distribution of proppant

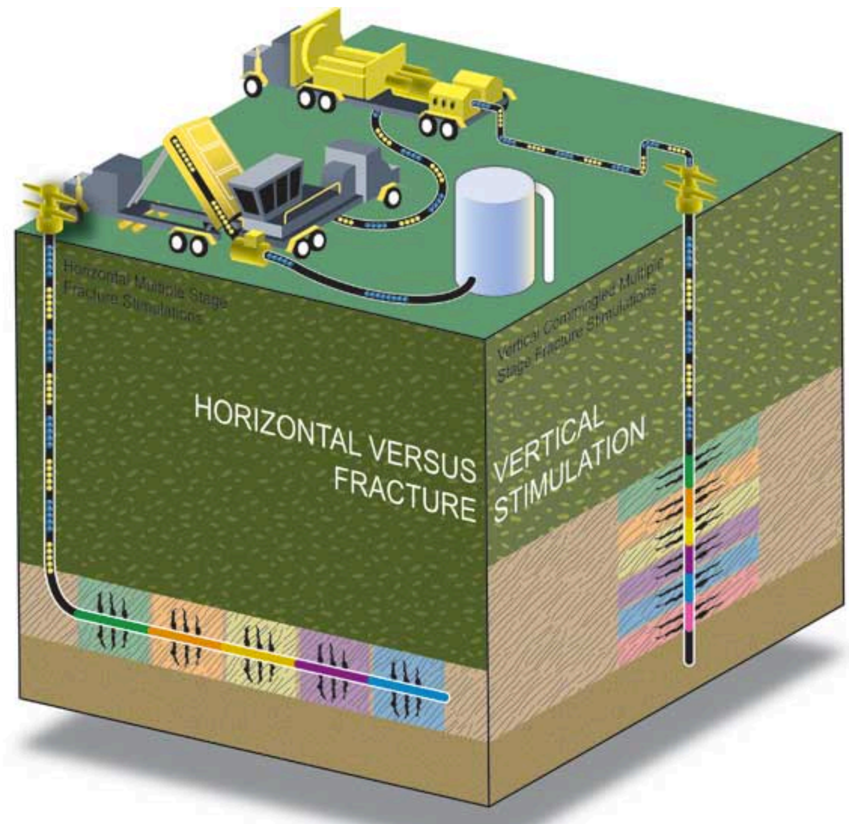

(National Energy Board, Canada, 2009)

Current Fracture Monitoring Techniques

- Far Well:
  - Microseismic
  - Tiltmeters
  - Pressure
  - Fiber Optics
- Near Well:
  - Logs
  - Tracers

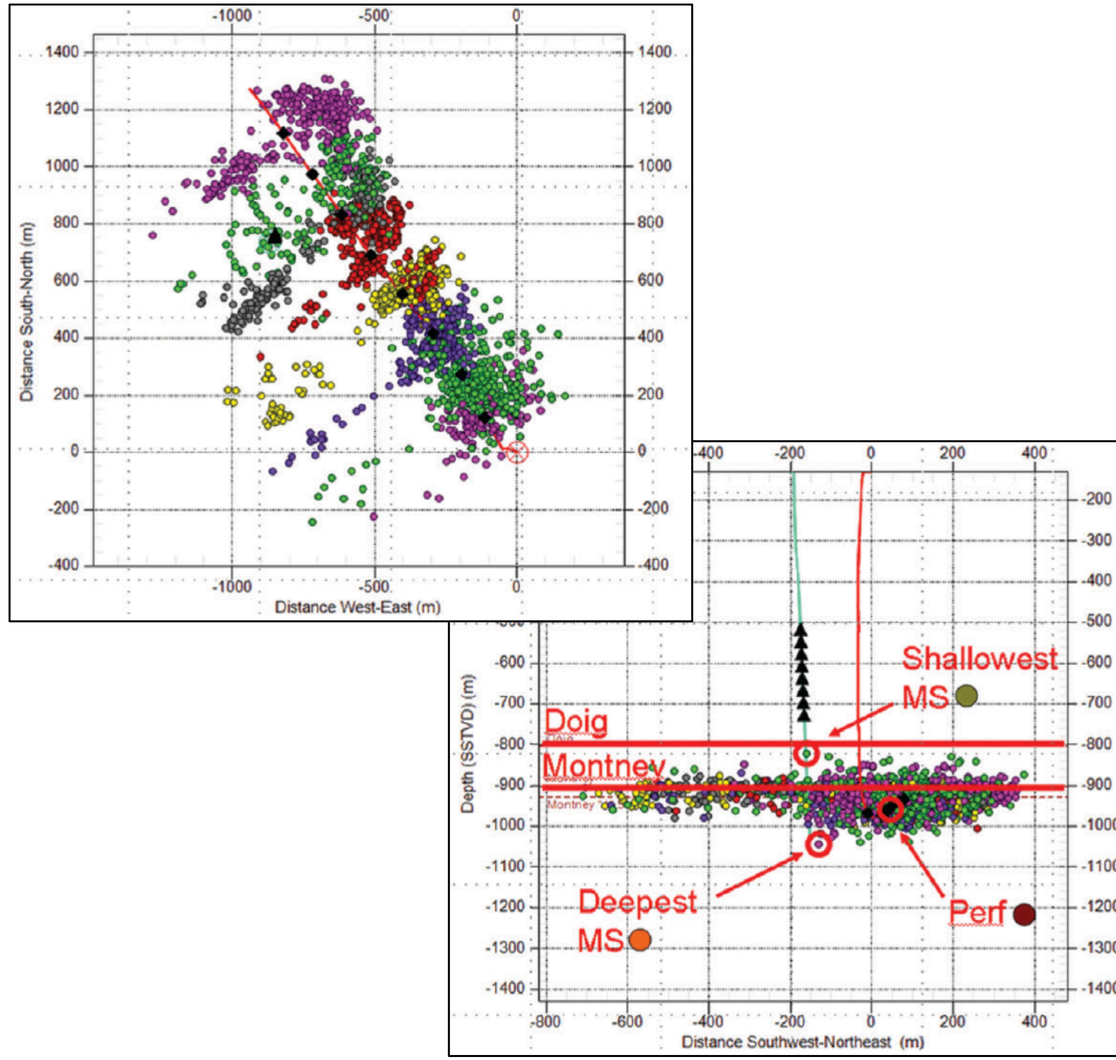

(Maxwell, 2011)

GIF

Schlumberger

Current Fracture Monitoring Techniques

- Far Well:
  - Microseismic
  - Tiltmeters
  - Pressure
  - Fiber Optics
- Near Well:
  - Logs
  - Tracers

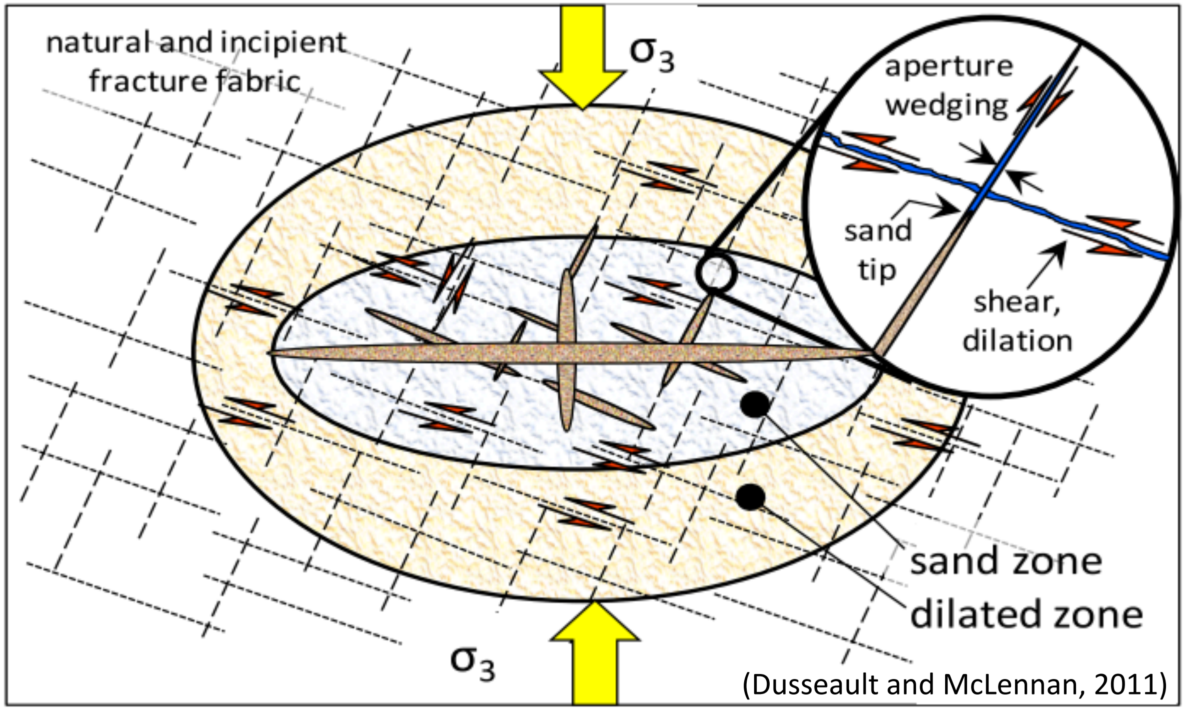

(Dusseault and McLennan, 2011)

Current Fracture Monitoring Techniques

- Far Well:
  - Microseismic
  - Tiltmeters
  - Pressure
  - Fiber Optics
- Near Well:
  - Logs
  - Tracers

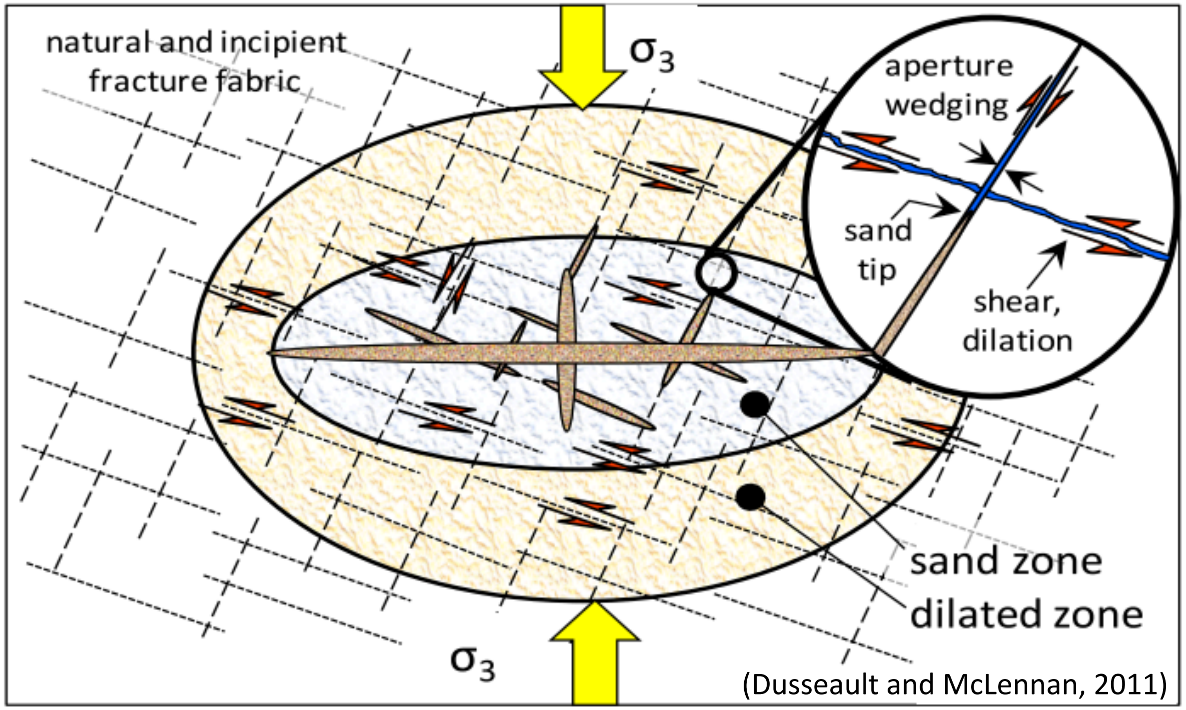

(Dusseault and McLennan, 2011)

Limited sensitivity to proppant distribution

Imaging the Propped Volume

Requirements:

1. Physical property contrast

2. Survey sensitive to contrast

3. Interpret / Invert data

Imaging the Propped Volume

Requirements:

1. Physical property contrast
2. Survey sensitive to contrast

Approach:

1. Electrically Conductive Proppant
2. Electromagnetic Survey

3. Interpret / Invert data

Physical Property Model

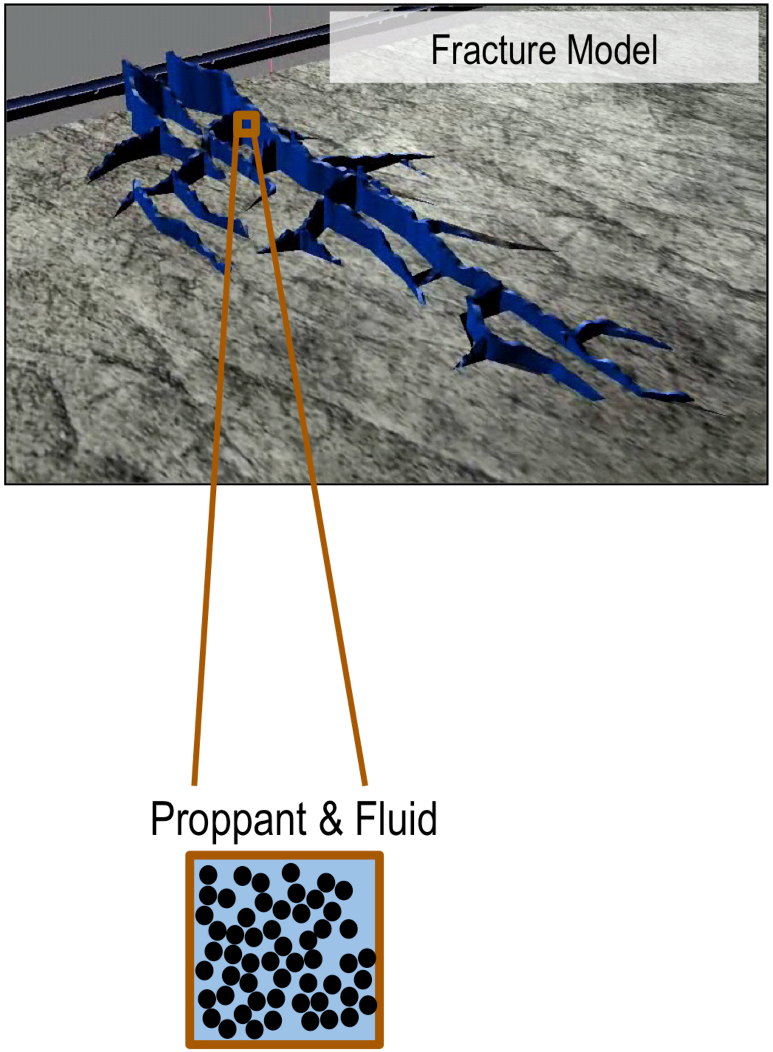

- What does a fracture look like as an electrical conductivity target?
- Scales:
  - Proppant: µm-mm
  - Fracture geometry
    - Length: 100’s m
    - Height: 10’s m
    - Width: µm-mm

Physical Property Model

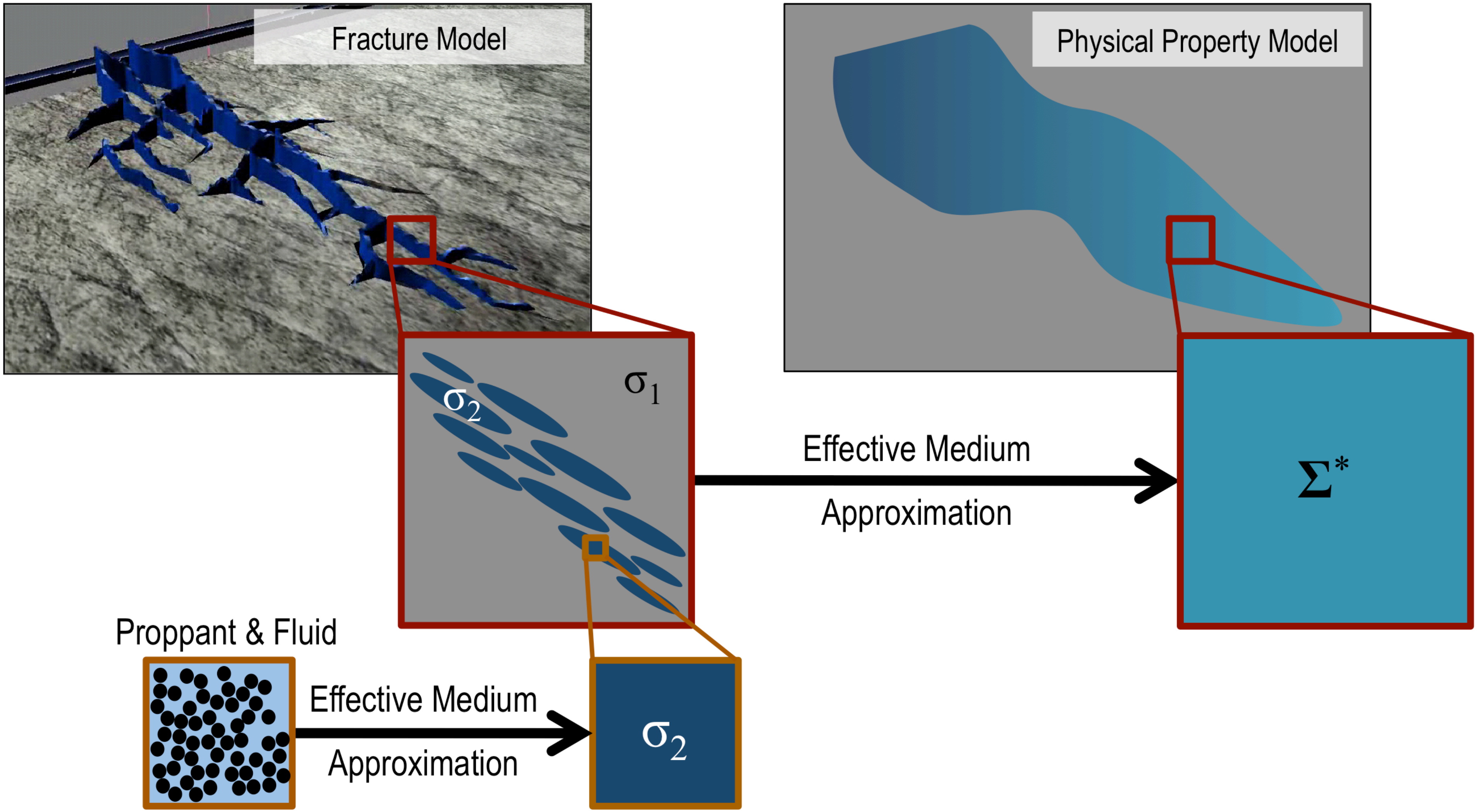

Schlumberger

Motivating Example

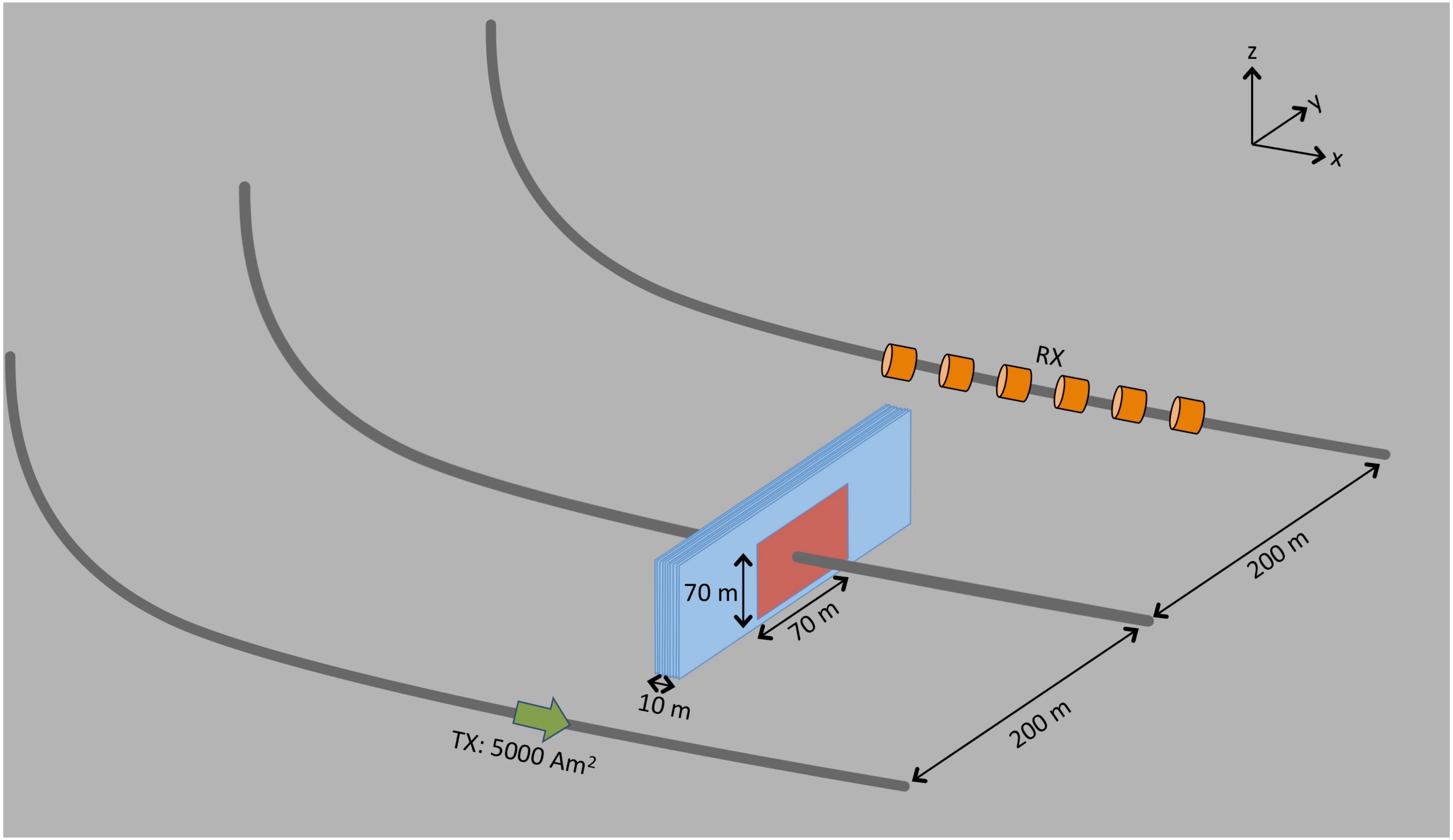

GIF

Schlumberger

Motivating Example

- 10 Fractures:
  - each 2.5mm wide
  - spaced evenly over 10m horizontal segment
- Propped Region:
  - 70x70m area
  - 50% proppant
  - 50% fluid

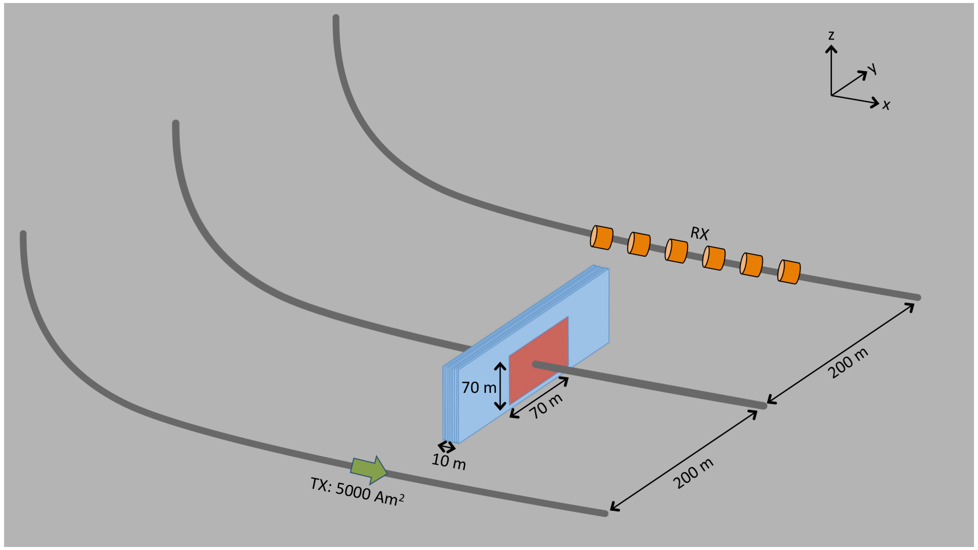

Characterizing the Physical Properties

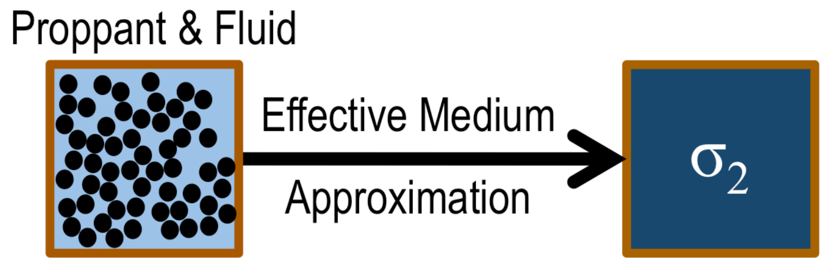

- Step 1:
  - Assume fractures filled with
    - conductive proppant
    - fluid
  - Compute σ_2 for a proppant-fluid mixture

Characterizing the Physical Properties

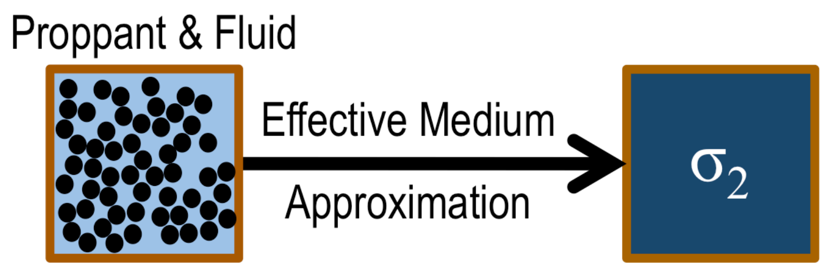

- Step 1:
  - Assume fractures filled with
    - conductive proppant
    - fluid
  - Compute σ_2 for a proppant-fluid mixture
  - Self consistent effective medium theory: spheres

$$\sum_{j=1}^{N} \phi_j (\sigma^* - \sigma_j) \mathrm{R}^{(j,*)} = 0$$

$$\mathrm{R}^{(j,*)} = \left[1 + \frac{1}{3} \frac{\sigma_j - \sigma^*}{\sigma^*} \right]^{-1}$$

Characterizing the Physical Properties

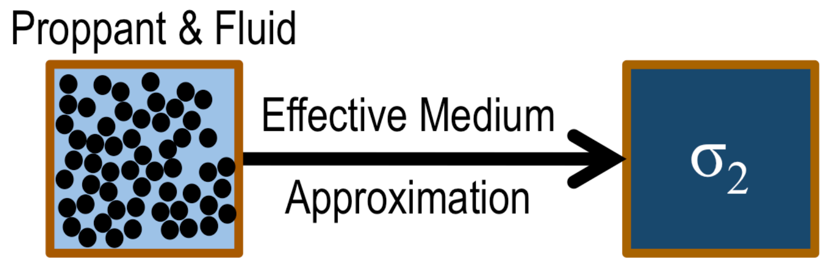

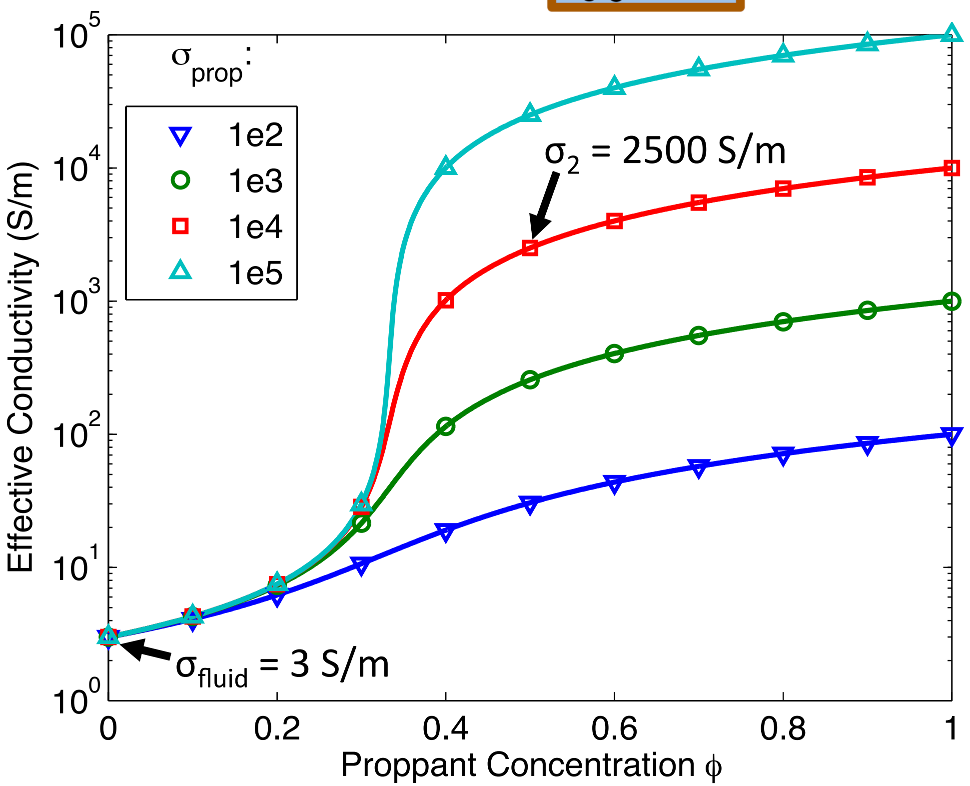

- Self consistent effective medium theory: spheres

$$\sum_{j=1}^{N} \phi_j (\sigma^* - \sigma_j) \mathrm{R}^{(j,*)} = 0$$

$$\mathrm{R}^{(j,*)} = \left[1 + \frac{1}{3} \frac{\sigma_j - \sigma^*}{\sigma^*} \right]^{-1}$$

Characterizing the Physical Properties

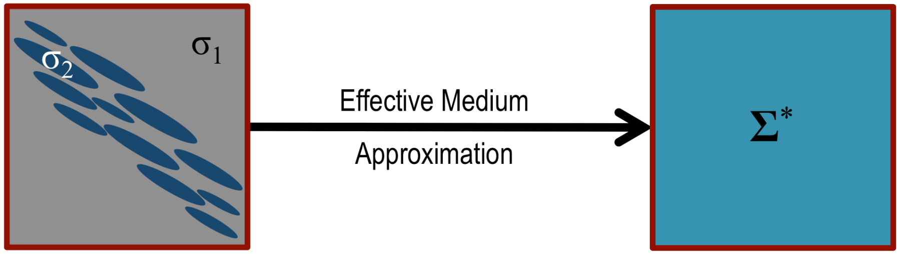

- Step 2:
  - Approximate fractures reservoir
    - aligned ellipsoidal cracks
    - background
  - Compute Σ^* for a propped, fractured volume of rock

Characterizing the Physical Properties

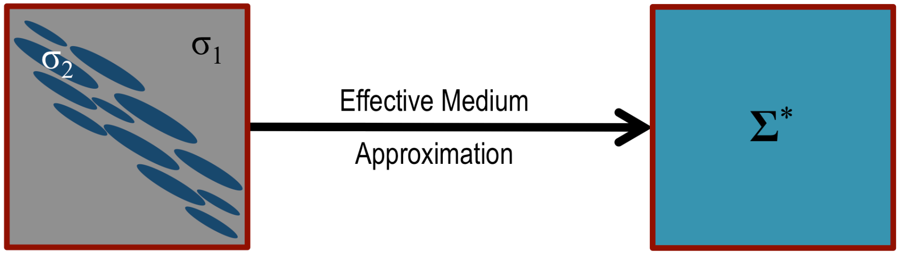

- Step 2:
  - Approximate fractures reservoir
    - aligned ellipsoidal cracks
    - background
  - Compute Σ^* for a propped, fractured volume of rock
  - Self consistent effective medium theory: aligned ellipsoids

$$\sum_{j=1}^{N} \phi_j (\mathbf{\Sigma}^* - \sigma_j \mathbf{I}) \mathbf{R}^{(j,*)} = 0$$

$$\mathbf{R}^{(j,*)} = \left[\mathbf{I} + \mathbf{A}_j \mathbf{\Sigma}^{*-1} (\sigma_j \mathbf{I} - \mathbf{\Sigma}^*) \right]^{-1}$$

Characterizing the Physical Properties

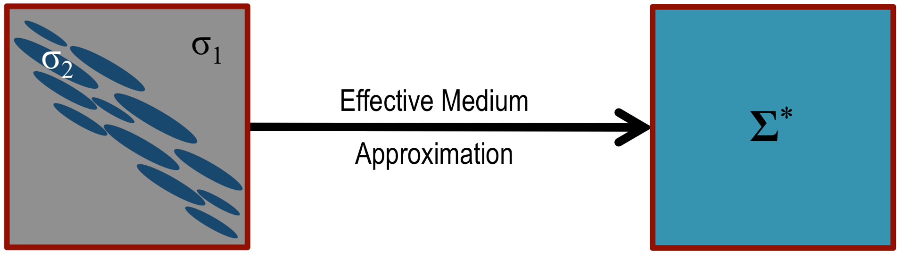

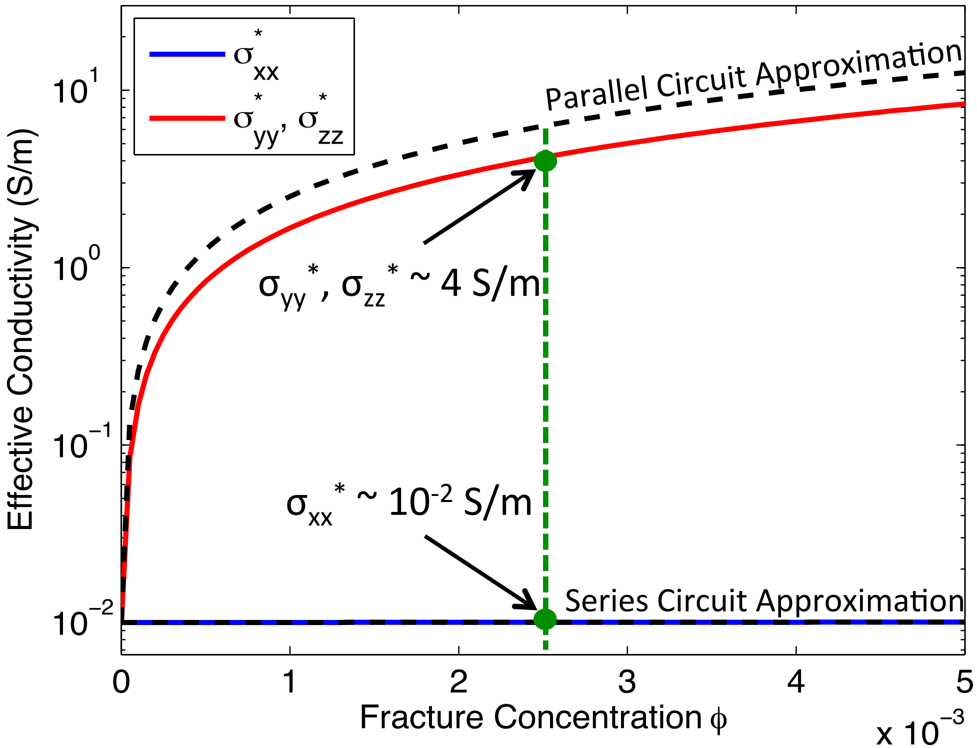

– Self consistent effective medium theory: aligned ellipsoids

$$\sum_{j=1}^{N} \phi_j (\mathbf{\Sigma}^* - \sigma_j \mathbf{I}) \mathbf{R}^{(j,*)} = 0$$

$$\mathbf{R}^{(j,*)} = \left[\mathbf{I} + \mathbf{A}_j \mathbf{\Sigma}^{*\,-1} (\sigma_j \mathbf{I} - \mathbf{\Sigma}^*) \right]^{-1}$$

Motivating Example

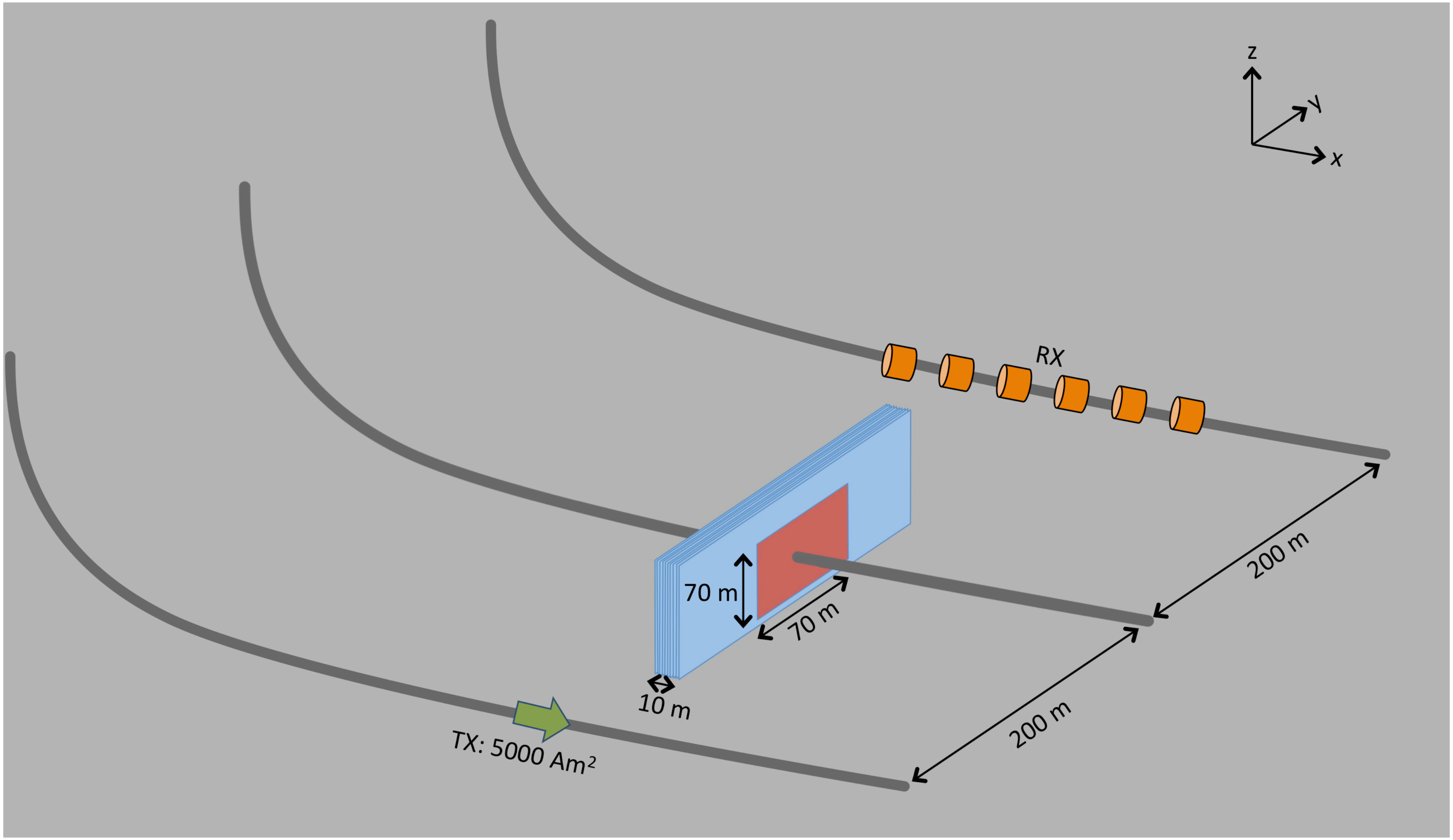

Motivating Example

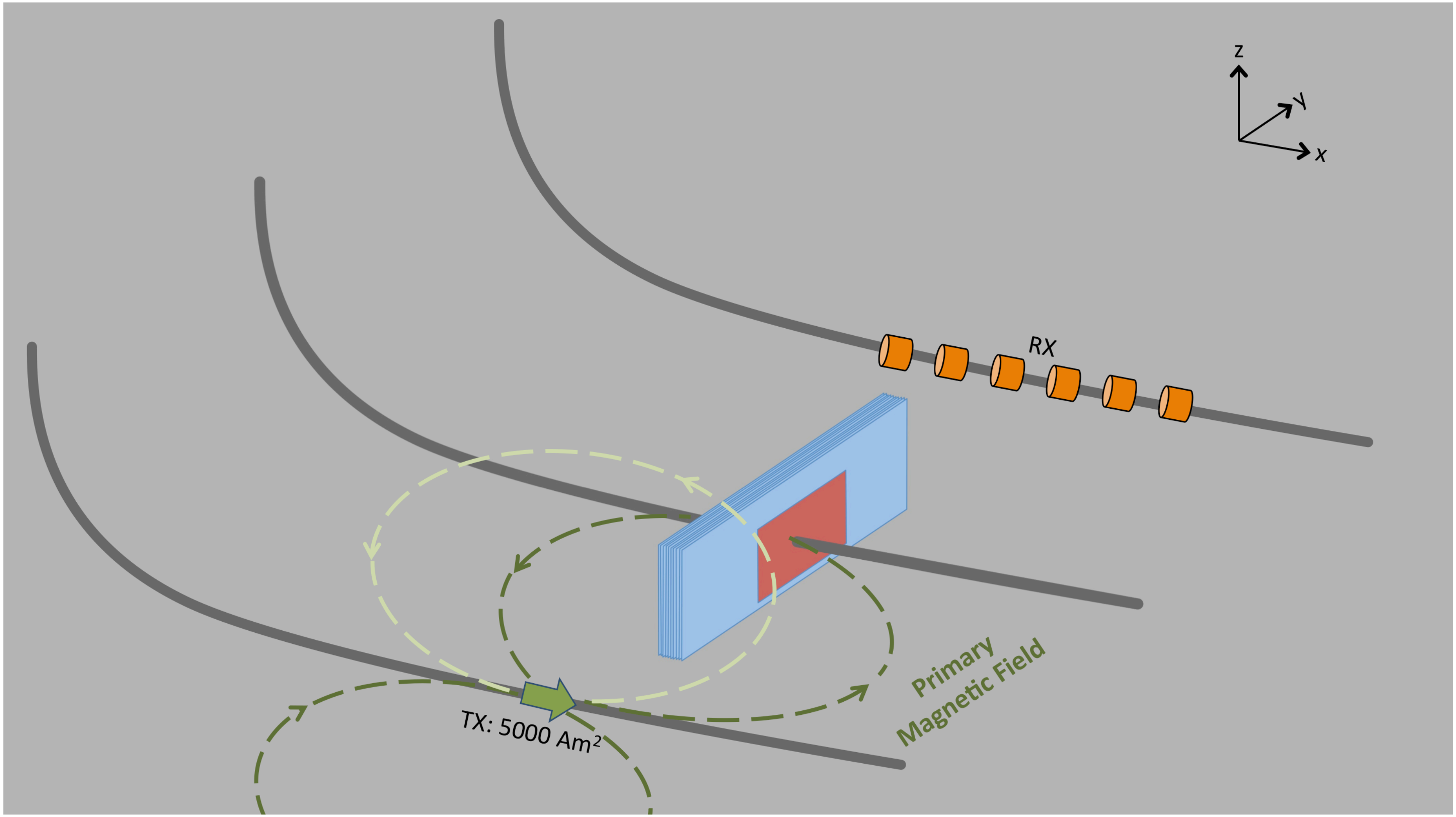

Motivating Example

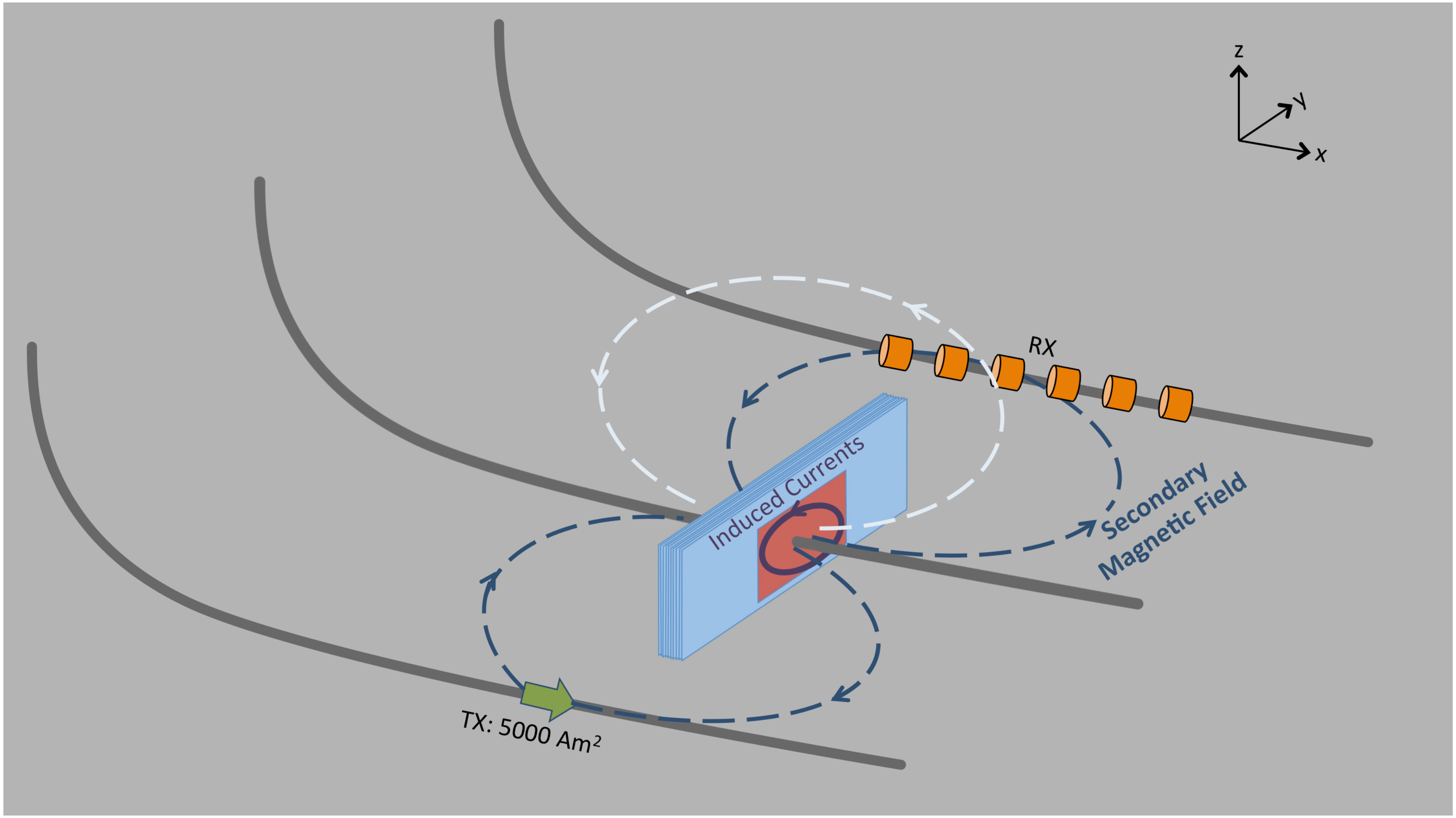

Magnetic Responses

- Measurements:
  - TX Frequency Range: 10Hz to 2kHz
  - In-phase and quadrature
  - 3 spatial components: x,y,z
- To detect fracture:
  - Signal & Secondary above RX noise floor
    - 10^{-2} pT
  - Secondary a sufficient percentage of primary

In-Phase, Bx component

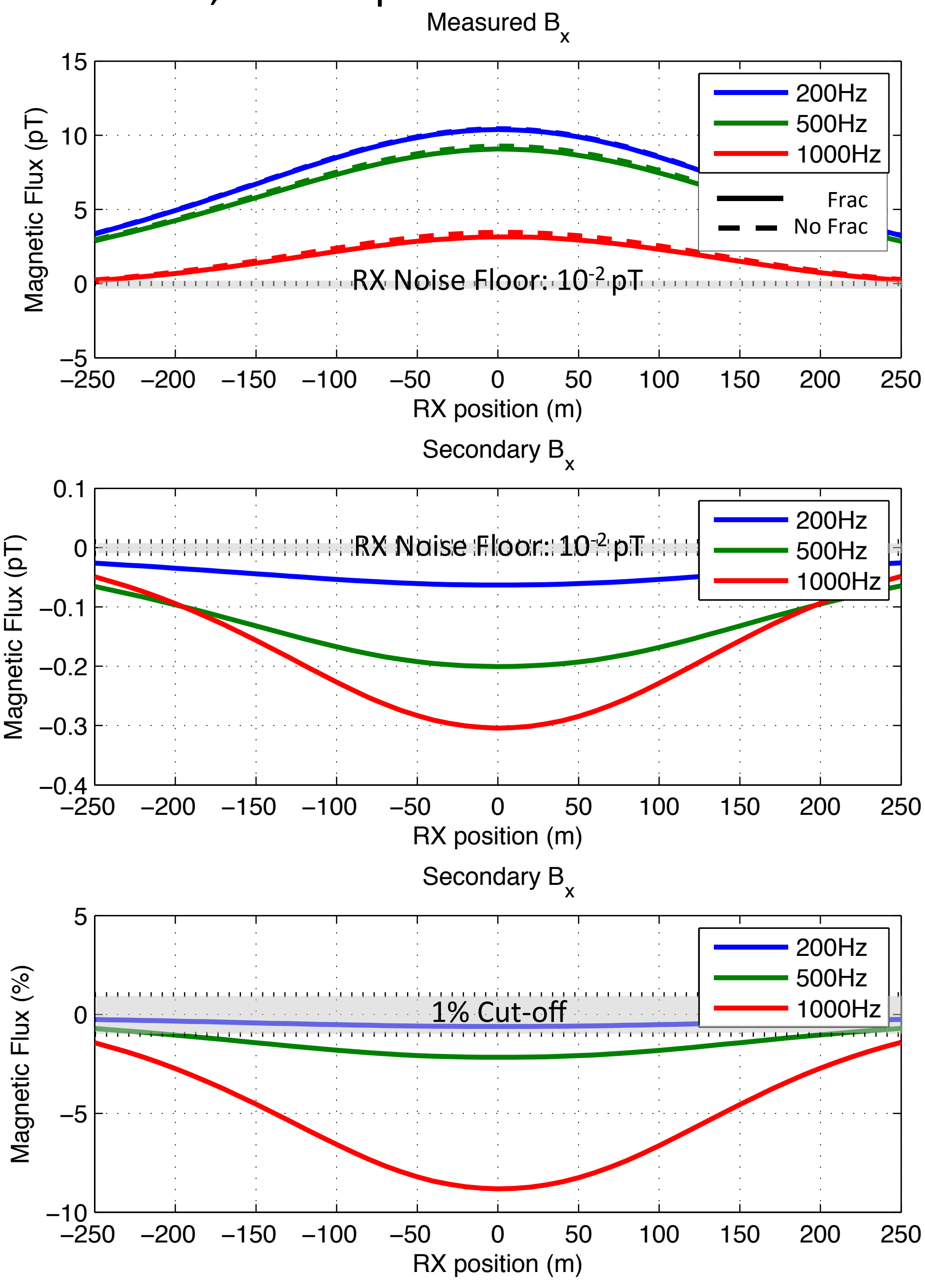

Magnetic Responses

- Measurements:
  - TX Frequency Range: 10Hz to 2kHz
  - In-phase and quadrature
  - 3 spatial components: x,y,z
- To detect fracture:
  - Signal & Secondary above RX noise floor
    - 10^{-2} pT
  - Secondary a sufficient percentage of primary

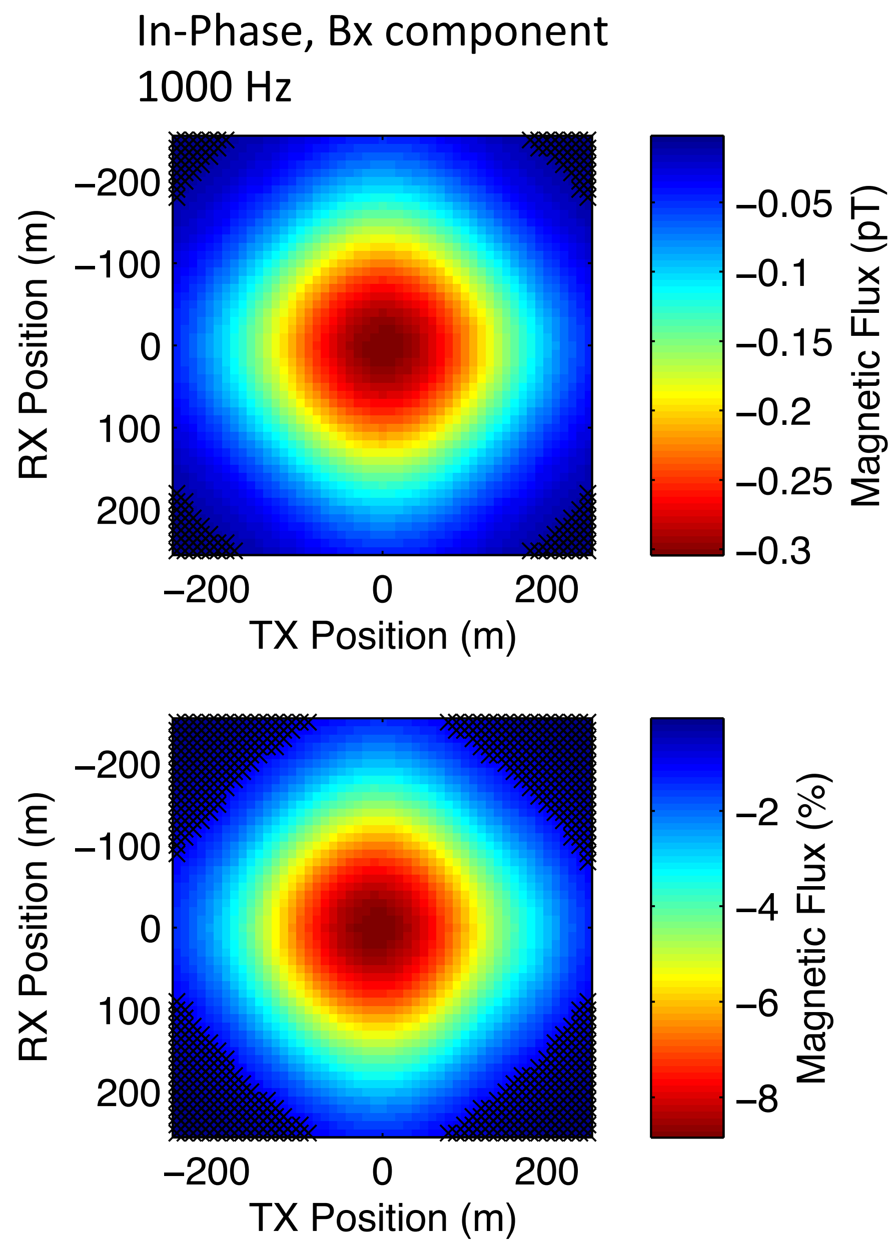

Summary & Outlook

- Physical property contrast: electrically conductive proppant

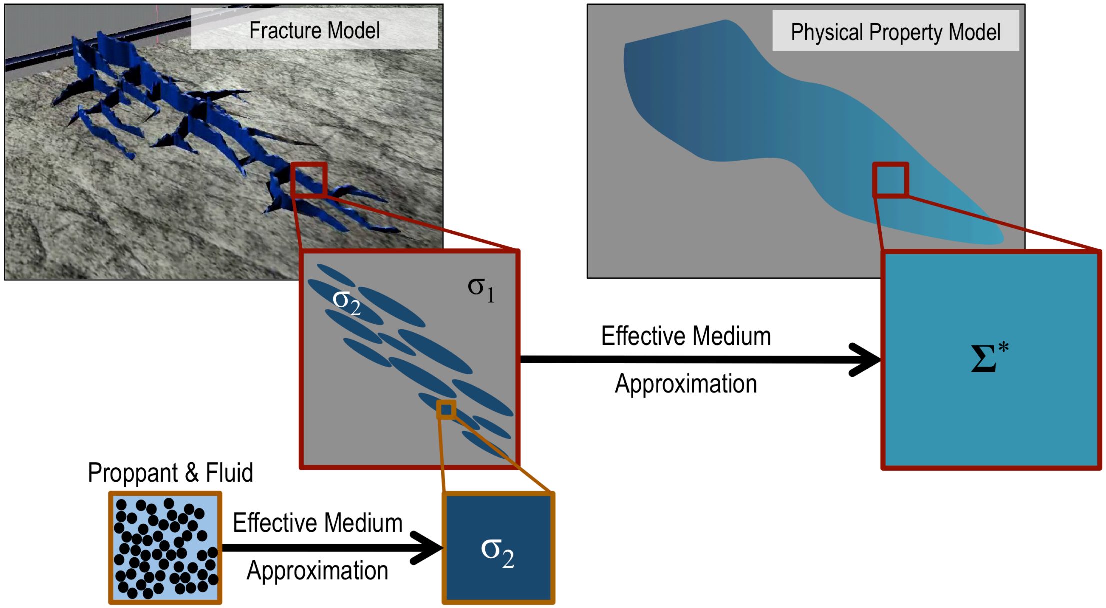

- Forward-modeled results: signal above RX noise level and is significant in percentage of the primary

Summary & Outlook

- Moving forward:
  - increase complexity of models
  - examine the survey design
  - invert the 3D electromagnetic data

1. Electrically Conductive Proppant
2. Electromagnetic Survey
3. Interpret / Invert data

Goal: to ascertain under what conditions EM imaging can provide cost effective information about proppant distribution in a fractured reservoir.

Acknowledgements

- Thanks to Nestor Cuevas and Ping Zhang for their contributions to this project
- Thanks to Christoph Schwarzbach for the forward modeling code

Thank you!

Questions?

References

- Berryman, J. G. & Hoversten, G. M. Modelling electrical conductivity for earth media with macroscopic fluid-filled fractures. *Geophys. Prospect.* **61,** 471–493 (2013).
- Bruggeman, D. A. G. The calculation of various physical constants of heterogeneous substances. I. The dielectric constants and conductivities of mixtures composed of isotropic substances. *Ann. Phys.* **416,** 636–664 (1935).
- Cipolla, C. L., Warpinski, N. R., Mayerhofer, M. J. & Technologies, P. SPE 115771 Hydraulic Fracture Complexity : Diagnosis , Remediation , and Exploitation. 20–22 (2008).
- Dusseault, M., & McLennan, J. (2011). Massive multi-stage hydraulic fracturing: Where are we?. *ARMA (American Rock Mechanics Association) e-Newsletter. Published*, *1*, 2011.
- Maxwell, S.C., Hydraulic fracture height growth. Recorder **36,** 18-22 (2011)
- Shafiro, B. & Kachanov, M. Anisotropic effective conductivity of materials with nonrandomly oriented inclusions of diverse ellipsoidal shapes. *J. Appl. Phys.* **87,** 8561–8569 (2000).
- Torquato, S. *Random Heterogeneous Materials: Microstructure and Macroscopic Properties*. (Springer, 2002).
- Wilt, M. J. *et al.* Crosswell electromagnetic tomography: System design considerations and field results. *Geophysics* **60,** 871–885 (1995).
- http://www.neb-one.gc.ca/clf-nsi/archives/rnrgynfmtn/nrgyrprt/ntrlgs/prmrndrstndngshlgs2009/prmrndrstndngshlgs2009-eng.html

Fracture Geometries

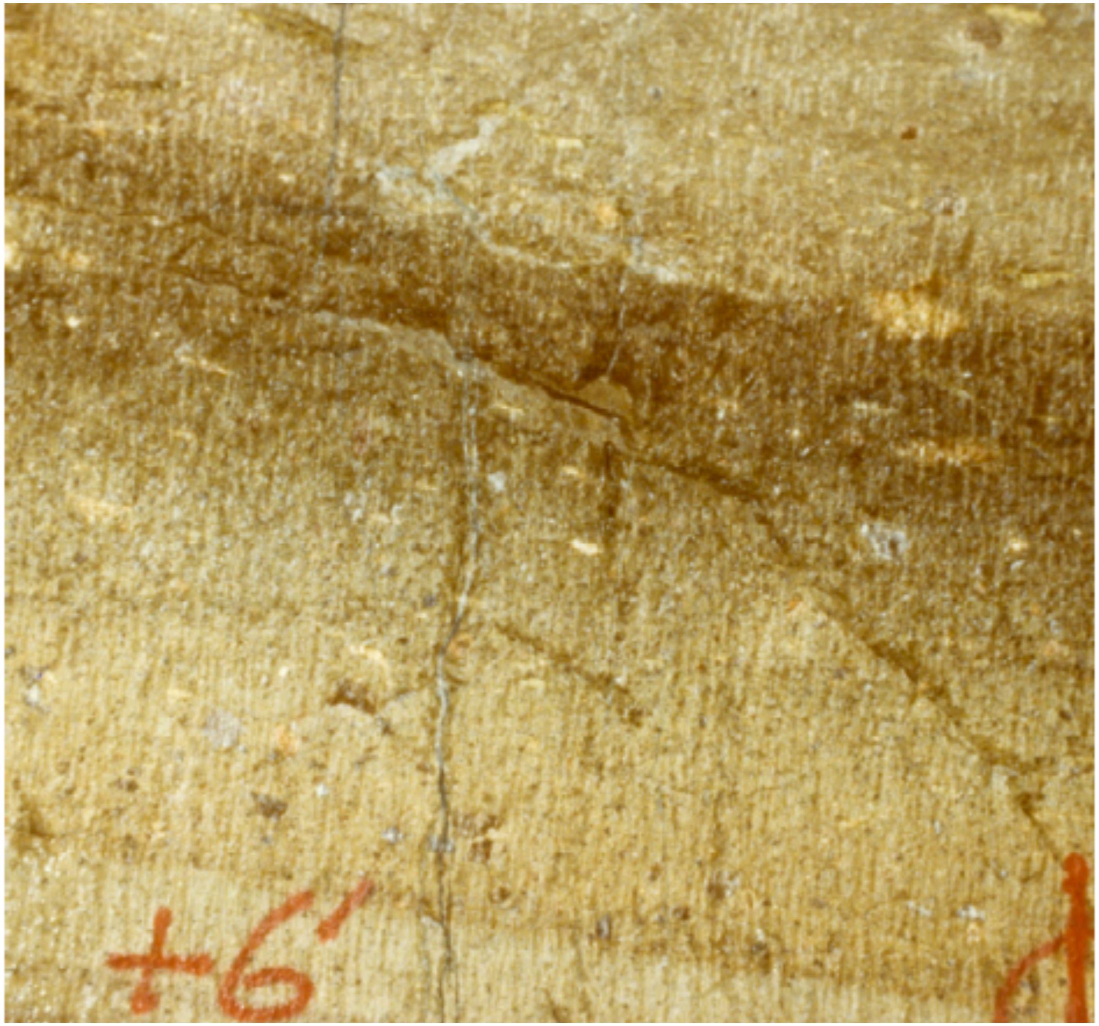

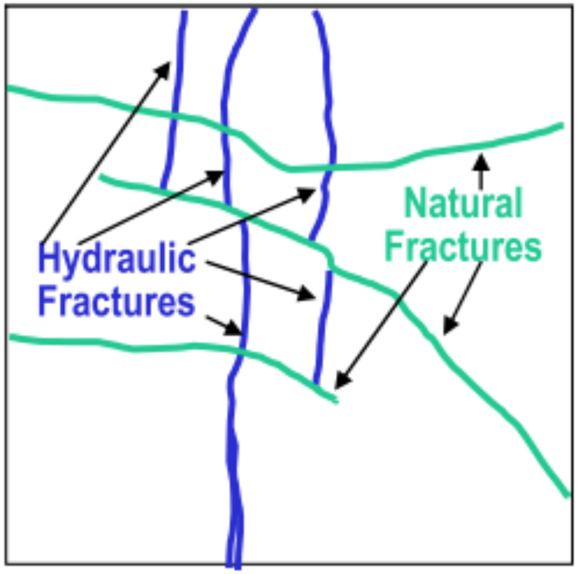

(Cipolla, 2008)

Fracture Geometries

Figure 7 – Example of complex vertical fracture growth from mine-back

Figure 8 – Photograph of a mostly single fracture that is non-planar, probably an impediment to proppant settling

(Cipolla, 2008)

Motivating Example

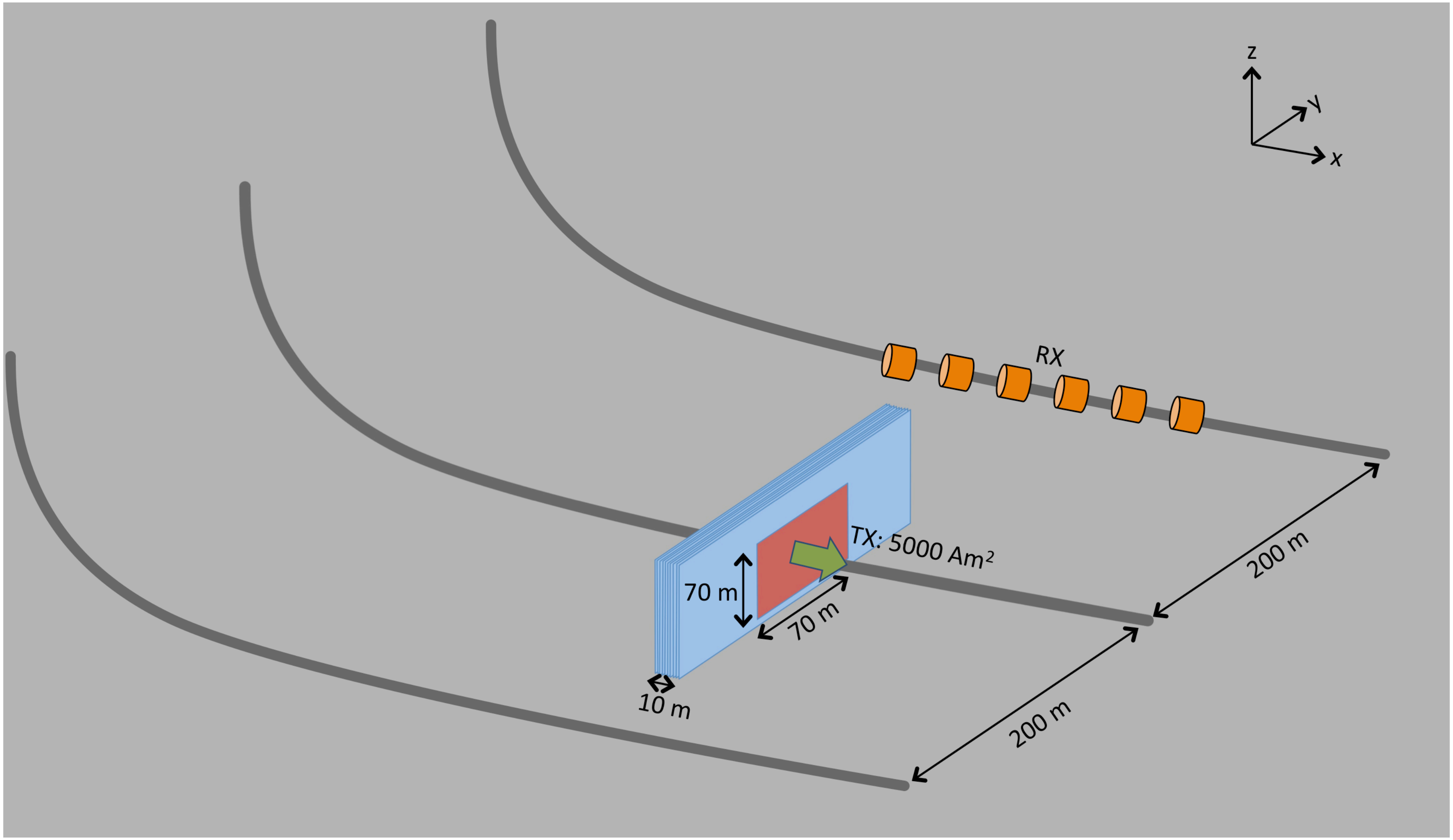

Magnetic Responses

- Measurements:
  - TX Frequency Range: 10Hz to 2kHz
  - In-phase and quadrature
  - 3 spatial components: x,y,z
- To detect fracture:
  - Signal & Secondary above RX noise floor
    - 10^{-2} pT
  - Secondary a sufficient percentage of primary

In-Phase, Bx component

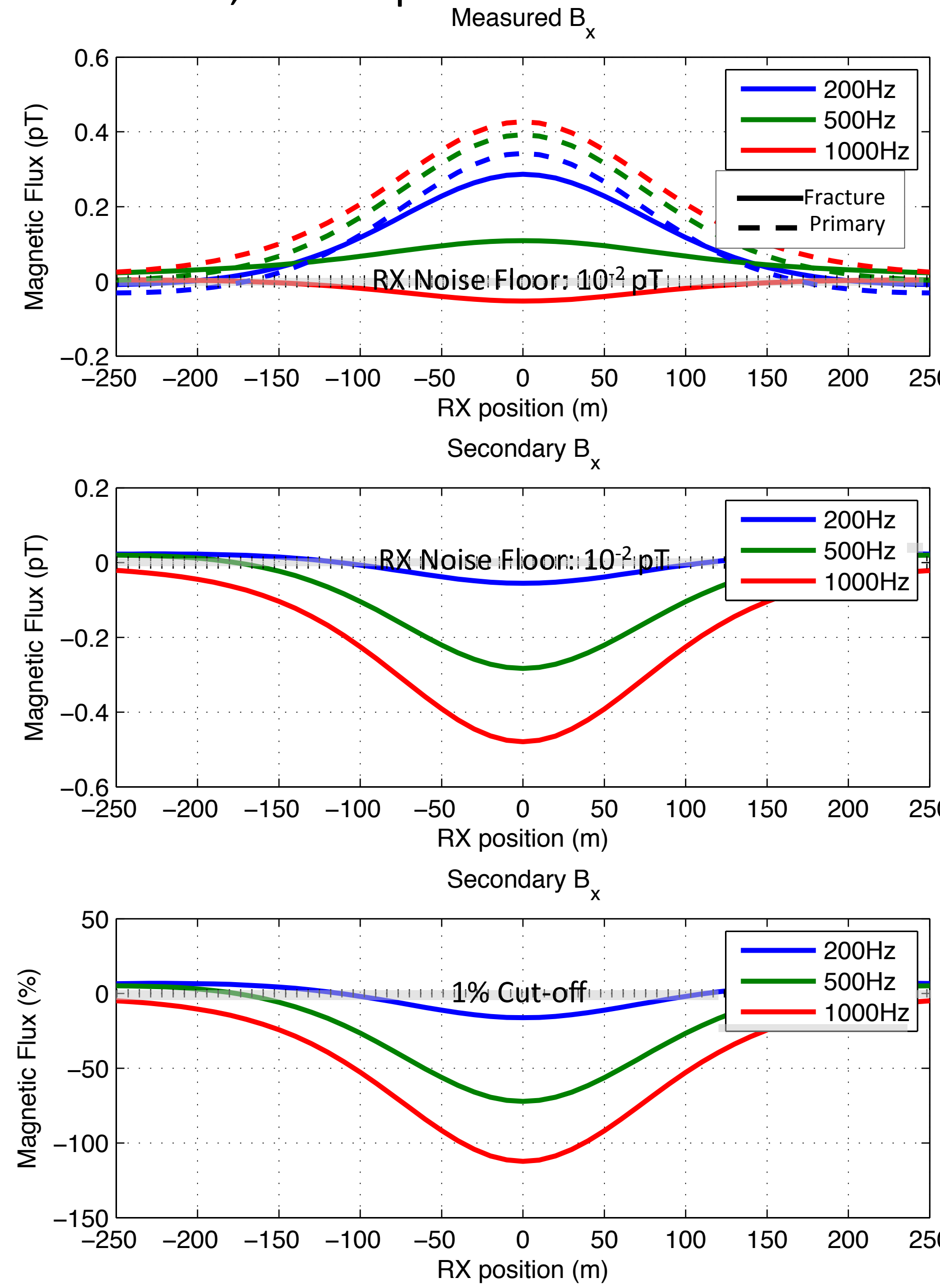

Magnetic Responses

- Measurements:
  - TX Frequency Range: 10Hz to 2kHz
  - In-phase and quadrature
  - 3 spatial components: x,y,z
- To detect fracture:
  - Signal & Secondary above RX noise floor
    - 10^{-2} pT
  - Secondary a sufficient percentage of primary

In-Phase, Bx component
1000 Hz

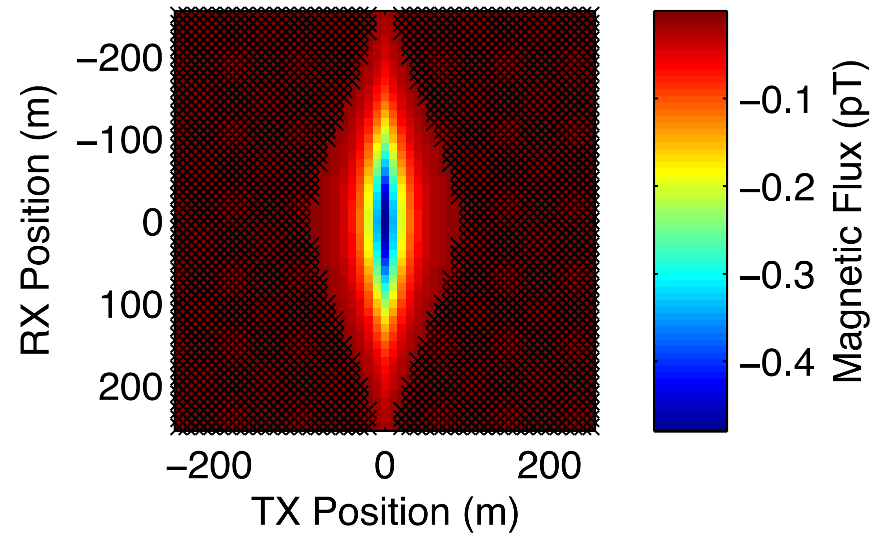

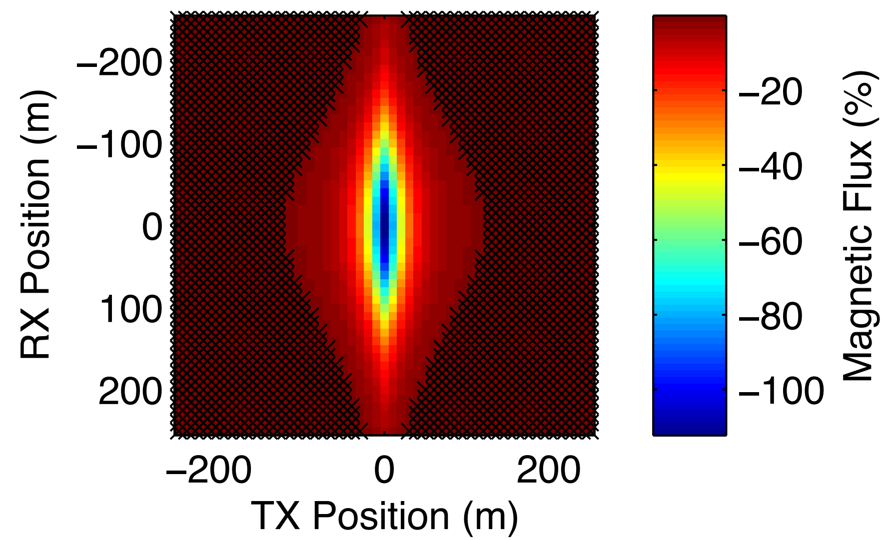

Single Inclusion Solutions

- Inside a sphere

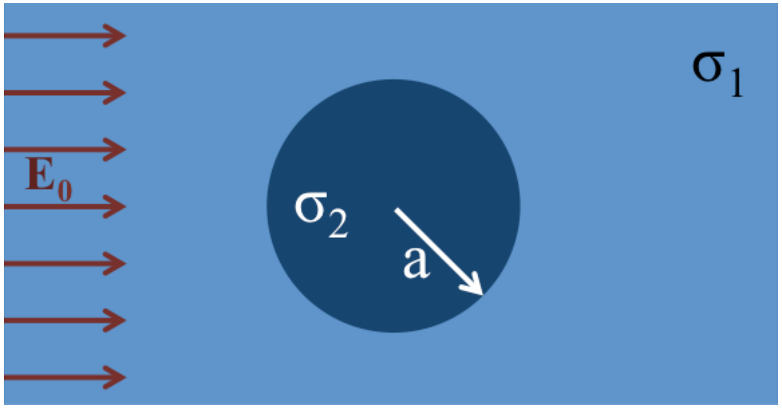

$$\mathbf{E} = \mathrm{R}^{(2,1)}\mathbf{E}_0$$

$$\mathrm{R}^{(2,1)} = \left[1 + \frac{1}{3}\frac{\sigma_2 - \sigma_1}{\sigma_1}\right]^{-1}$$

- Inside an Ellipsoid

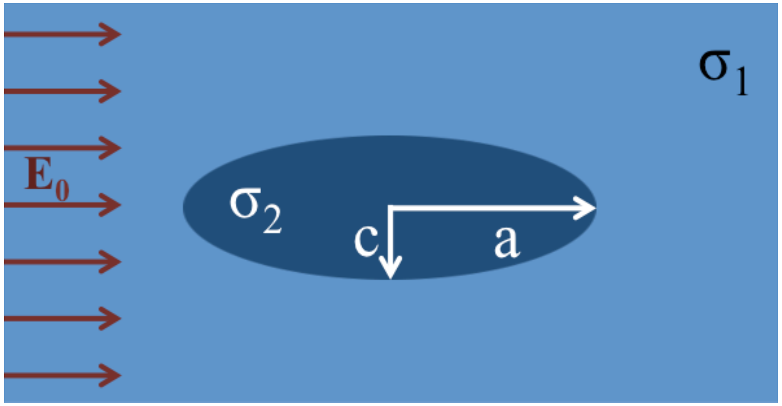

$$\mathbf{E} = \mathbf{R}^{(2,1)}\mathbf{E}_0$$

$$\mathbf{R}^{(2,1)} = \left[\mathbf{I} + \mathbf{A}_2\frac{\sigma_2 - \sigma_1}{\sigma_1}\right]^{-1}$$

Maxwell Approximation

- Spherical Inclusions
- Ellipsoidal Inclusions

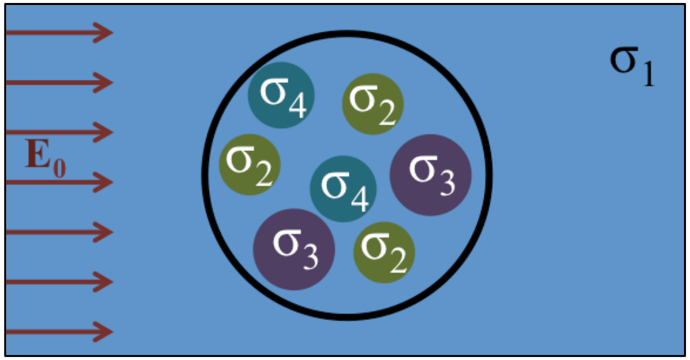

$$\sum_{j=1}^{N} \phi_j(\sigma^* - \sigma_j)\mathrm{R}^{(j,1)} = 0$$

$$\mathrm{R}^{(j,1)} = \left[1 + \frac{1}{3}\frac{\sigma_j - \sigma_1}{\sigma_1}\right]^{-1}$$

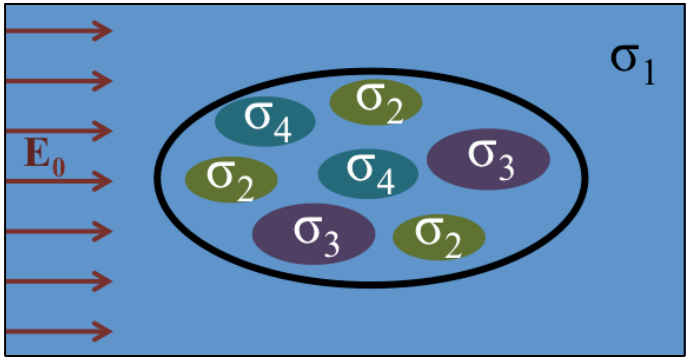

$$\sum_{j=1}^{N} \phi_j(\mathbf{\Sigma}^* - \sigma_j\mathbf{I})\mathbf{R}^{(j,1)} = 0$$

$$\mathbf{R}^{(j,1)} = \left[\mathbf{I} + \mathbf{A}_j\frac{\sigma_j - \sigma_1}{\sigma_1}\right]^{-1}$$

Self Consistent Approximation

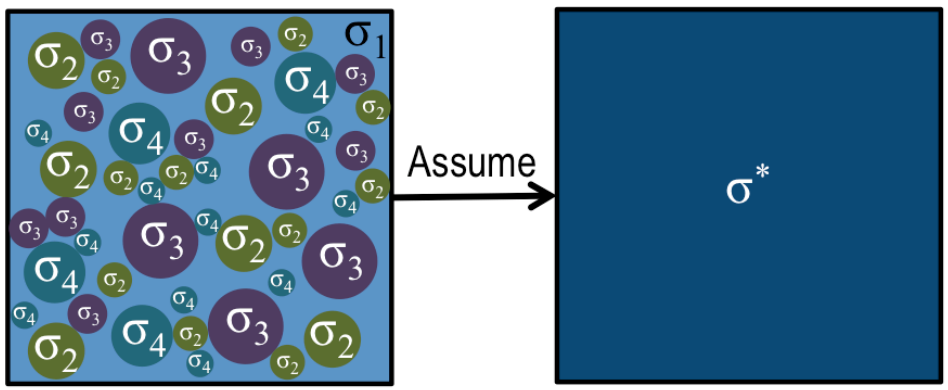

Spherical Inclusions

$$\sum_{j=1}^{N} \phi_j(\sigma^* - \sigma_j)\mathrm{R}^{(j,*)} = 0$$

$$\mathrm{R}^{(j,*)} = \left[1 + \frac{1}{3}\,\frac{\sigma_j - \sigma^*}{\sigma^*}\right]^{-1}$$

Ellipsoidal Inclusions

$$\sum_{j=1}^{N} \phi_j(\widetilde{\boldsymbol{\Sigma}}^* - \sigma_j\widetilde{\mathbf{I}})\widetilde{\mathbf{R}}^{(j,*)} = 0$$

$$\widetilde{\mathbf{R}}^{(j,*)} = \left[\widetilde{\mathbf{I}} + \widetilde{\mathbf{A}}_j\,\widetilde{\boldsymbol{\Sigma}}^{*\,-1}(\sigma_j\widetilde{\mathbf{I}} - \widetilde{\boldsymbol{\Sigma}}^*)\right]^{-1}$$

Self Consistent Approximation

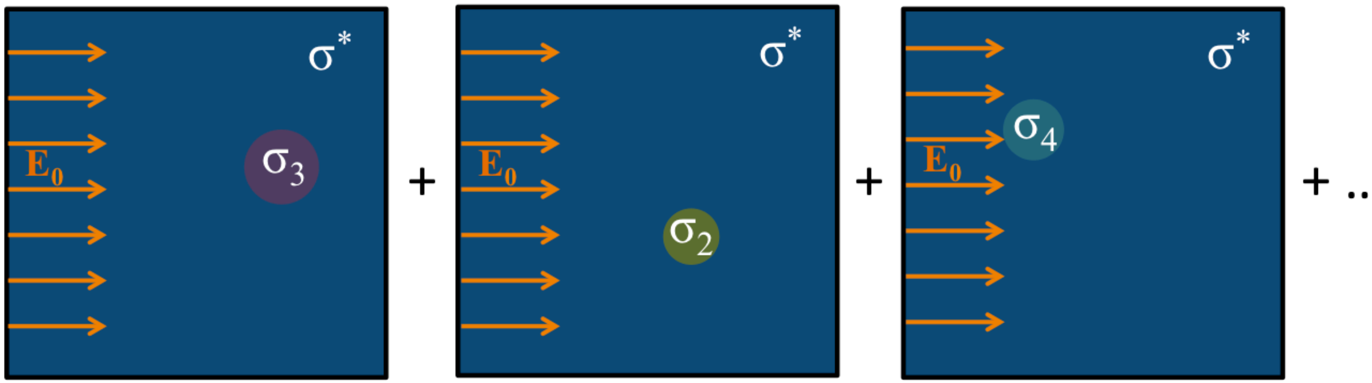

Spherical Inclusions

$$\sum_{j=1}^{N} \phi_j(\sigma^* - \sigma_j)\mathrm{R}^{(j,*)} = 0$$

$$\mathrm{R}^{(j,*)} = \left[1 + \frac{1}{3}\frac{\sigma_j - \sigma^*}{\sigma^*}\right]^{-1}$$

Ellipsoidal Inclusions

$$\sum_{j=1}^{N} \phi_j(\widetilde{\mathbf{\Sigma}}^* - \sigma_j\widetilde{\mathbf{I}})\widetilde{\mathbf{R}}^{(j,*)} = 0$$

$$\widetilde{\mathbf{R}}^{(j,*)} = \left[\widetilde{\mathbf{I}} + \widetilde{\mathbf{A}}_j\, {\widetilde{\mathbf{\Sigma}}^*}^{-1}(\sigma_j\widetilde{\mathbf{I}} - \widetilde{\mathbf{\Sigma}}^*)\right]^{-1}$$